

## N O T I C E

THIS DOCUMENT HAS BEEN REPRODUCED FROM  
MICROFICHE. ALTHOUGH IT IS RECOGNIZED THAT  
CERTAIN PORTIONS ARE ILLEGIBLE, IT IS BEING RELEASED  
IN THE INTEREST OF MAKING AVAILABLE AS MUCH  
INFORMATION AS POSSIBLE

(NASA-TM-80680) THE HEAO A-2 SURVEY OF  
ABELL CLUSTERS AND THE X-RAY LUMINOSITY  
FUNCTION (NASA) 42 p HC A03/MF A01 CSCL 03B

NO-28290

Unclas  
G3/93 25198



## Technical Memorandum 80680

# The HEAO A-2 Survey of Abell Clusters and the X-Ray Luminosity Function

J. D. McKee, R. F. Mushotzky,  
E. A. Boldt, S. S. Holt, F. E. Marshall,  
S. H. Pravdo, and P. J. Serlemitsos

APRIL 1980

National Aeronautics and  
Space Administration

Goddard Space Flight Center  
Greenbelt, Maryland 20771





Technical Memorandum 80680

# **The HEAO A-2 Survey of Abell Clusters and the X-Ray Luminosity Function**

**J. D. McKee, R. F. Mushotzky,  
E. A. Boldt, S. S. Holt, F. E. Marshall,  
S. H. Pravdo, and P. J. Serlemitsos**

**APRIL 1980**

National Aeronautics and  
Space Administration

**Goddard Space Flight Center**  
Greenbelt, Maryland 20771

THE HEAO A-2 SURVEY OF ABELL CLUSTERS AND THE  
X-RAY LUMINOSITY FUNCTION

J.D. McKee<sup>1</sup>, R.F. Mushotzky<sup>1</sup>, E.A. Boldt, S.S. Holt,  
F.E. Marshall, S.H. Pravdo<sup>2</sup>, and P.J. Serlemitsos

Laboratory for High Energy Astrophysics  
NASA/Goddard Space Flight Center  
Greenbelt, Maryland 20771

ABSTRACT

We have examined the HEAO A-2<sup>+</sup> all sky data base for 2-10 keV X-ray emission from the 225 Abell clusters of galaxies listed in Abell's (1958) catalog which are of distance class four or less, and are within the fraction of the sky surveyed completely by Abell. Thirty-two identifications of clusters with X-ray sources were made, for which we present 2-10 keV fluxes and 90% error boxes; twelve of these identifications are new. We have derived the X-ray luminosity function for this statistically complete sample, and have found the best exponential fit (between  $0.5 \times 10^{44}$  erg s<sup>-1</sup> and  $10^{45}$  ergs<sup>-1</sup>) to be  $f(L) = 20.2 \times 10^{-8} \exp (-L_{44}/1.9)$  per Mpc<sup>3</sup> per  $10^{44}$  erg s<sup>-1</sup> per 2-10 keV. The relationship between X-ray luminosity and richness has also been examined and a correlation has been found for richness classes 0, 1, and 2. We have also looked at the relationship of X-ray luminosity, Bautz-Morgan type, and Rood-Sastry type and have found that BM Type I's and RS type cD and B have the greatest average luminosity. The contribution of clusters to the X-ray background has been calculated from the luminosity function and has been found to be 5%, and with 90% certainty, less than 8% in the 2-10 keV band pass.

---

<sup>1</sup>Also Dept. of Physics and Astronomy, Univ. of Maryland

<sup>2</sup>Now with CIT

\*The A-2 experiment on HEAO-1 was a collaborative effort led by E. Boldt of GSFC and G. Garmire of CIT with collaborators at GSFC, CIT, JPL and UCB.

## I. INTRODUCTION

Clusters of galaxies have been of considerable interest as X-ray sources since Gursky et al. (1971,1972) first reported that rich Abell clusters have X-ray luminosities as high as  $10^{45}$  erg s<sup>-1</sup>. Since then many of the optically unidentified high galactic latitude objects detected with Uhuru and later satellites have been identified as clusters of galaxies, and rich clusters are now universally recognized as an important class of X-ray emitting objects. It is therefore highly desirable to survey as large and as unbiased a sample of clusters as possible in order to accurately determine cluster properties and their inter-relationships. The HEAO A-2 survey is the largest statistically complete X-ray survey done to date.

The survey is drawn from Abell's (1958) catalog of rich clusters of galaxies, and comprises all clusters in the catalog which are of distance class four or less ( $z \lesssim 0.1$ ), and are within the 4.65 steradians of the sky surveyed completely by Abell. There are 225 clusters which meet these criteria. We have searched the HEAO A2 all sky data base for 2-10 keV X-ray emission from each of these clusters, and report on twelve new identifications, as well as on the correlation of the cluster X-ray luminosities with BM type and richness, and present a new X-ray luminosity function for Abell clusters.

## II. THE EXPERIMENT

The HEAO A-2 experiment consisted of six mechanically collimated proportional counters spanning 2-60 keV in spectral response. The detectors scanned a great circle in the sky every half hour while the spin axis remained continually pointed at the sun. In this manner the entire sky was scanned in the course of a year as the great circle scans precessed one degree per day (see Rothschild et al. 1978 for a detailed description of the instrument). The fluxes which we

report here were obtained using the  $1\frac{1}{2}^\circ \times 3^\circ$  field-of-view collimator and are given in "R15" units, a term defined by Marshall et al. (1979). An R15 unit is about 1 Uhuru flux unit, but the exact conversion to UFU's is spectrally dependent since the R15 unit comprises the 4-17 keV band at half efficiency, while the Uhuru flux unit corresponds to 2-6 keV. Specifically, in terms of  $\text{erg cm}^{-2} \text{s}^{-1}$ , an X-ray source described by a power law with photon index  $\alpha = 1.5$  gives 1 R15 count per second per  $2.1 \times 10^{-11} \text{ erg cm}^{-2} \text{s}^{-1}$  in the 2-10 keV band. For thermal bremsstrahlung sources (such as clusters, presumably) 1 R15 count per second corresponds to  $2.8 \times 10^{-11} \text{ erg cm}^{-2} \text{s}^{-1}$  in the 2-10 keV band if  $kT = 4 \text{ keV}$ ,  $2.5 \times 10^{-11}$  if  $kT = 7 \text{ keV}$ , and  $2.1 \times 10^{-11} \text{ erg cm}^{-2} \text{s}^{-1}$  if  $kT = 9 \text{ keV}$ . Most known clusters sources fall within the range  $kT \sim 4\text{-}9 \text{ keV}$  (OSO-8 survey; Mushotzky et al. 1979). We do not as yet have temperatures for all the clusters we have observed, and have therefore assumed  $kT = 7 \text{ keV}$  in order to convert R15 counts to approximate fluxes and luminosities. The maximum systematic error in the flux incurred by this assumption is 20% if the cluster  $kT$  is within the 4-9 keV range observed with OSO-8. The  $1\sigma$  counting statistics error is smaller, however, being typically 0.2 R15 counts per second.

### III. OBSERVATIONS

#### a. Selection Criteria and Error Boxes

The survey sample consists of all clusters of distance class four or less which are within the fraction of the sky surveyed completely by Abell (1958). This implies that the clusters are at galactic latitudes of absolute value greater than  $20^\circ$ , declinations more northerly than  $-20^\circ$ , and  $z$ 's greater than 0.01. The sample differs from Abell's (1958) "statistical sample" only in the inclusion of richness class zero clusters and the cut-off at distance class four. It is desirable to include richness class zero clusters since these determine the low-luminosity behavior of the luminosity function. Richness class zero clusters are certainly not completely identified for distance classes 5 and 6, but probably are for distance class four and less. This is evidenced by the fact that the fraction of clusters in a given distance class which are richness class zero clusters is nearly constant in our sample: the fraction is 0.41, 0.46, and 0.57 for distance

classes 1+2, 3 and 4 respectively. The optical data base is probably not unduly biased, therefore, by the inclusion of the  $R=0$  clusters. The X-ray data base was searched for evidence of emission from the 225 clusters which meet the criteria described above. The A-2 data base consists of the sum of several days' overlapping great circle scans of a given position in the sky. In order for an X-ray source to be considered as real, we have required that a point source model of the collimator response decrease  $\chi^2$  by 11.0 as compared to a uniform sky model. The probability that a source that meets this requirement is spurious, is 0.005. Thus with 225 cluster candidates, the number of possibly spurious sources is 1.1. The source position is determined in terms of a scan angle, and a coordinate orthogonal to this, and then transformed to R.A. and dec. The 95% error interval in the scan angle is obtained by observing how far the source must be displaced from the best fit position to cause an increase in  $\chi^2$  of 6.2. (Intensity and background are treated as free parameters when the source is displaced. The procedure follows that of Lampton, Margon and Bowyer 1976). The position coordinate orthogonal to the scan angle is obtained by modeling the data one day at a time and looking for a triangular response to the source as the day on which the source is centered approaches and recedes. This data is modeled and a position and a 95% error interval is obtained as above. The 95% error intervals combine to define a 90% error box. We have required that the associated cluster lie within this error box in order to be identified with the X-ray source.

An error box such as defined above can be made for sources of intensities greater than 0.3 R15 counts per second but all of the claimed detections in this paper have fluxes  $> 0.5$  R15 units. Below this sensitivity limit (0.3), the  $\chi^2$  fit to a point source differs by less than 6.2 from the fit obtained with background alone. Our survey limit is defined by source confusion, however, rather than sensitivity. The log N - log S curve derived from the HEAO A-2 data is given by  $N(>S) \approx 12.0 \text{ s}^{-3/2} \text{ sr}^{-1}$  (with S in R15 units), and predicts 158

sources brighter than 0.5 R15 counts within the area covered by the survey (4.65 sr). The average size of an x-ray error box in Table 2 is 1.2 square degrees. Thus for 225 clusters, we would expect, by chance, to make N false identifications where N is given by

$$N = (225 \times 1.2^0 / 4.65 \text{ sr}) \cdot 158 = 2.8$$

For a minimum flux of 0.7 the number of expected coincidences drops to 1.6. We have used 0.5 as the confusion limit and required that the cluster fluxes exceed this in order to identified as x-ray sources. Our statistical sample consists of clusters brighter than 0.7 R15, however, which is the completeness limit (see below).

b. Results

The results of the observations are listed in Table 1. Column one contains the Abell number, column two is the count rate in R15 units with  $1\sigma$  error, column three is the 2-10 keV X-ray luminosity expressed in units of  $10^{44}$  erg s<sup>-1</sup> and obtained by assuming kT = 7 keV; column four lists the cluster redshifts, columns five, six and seven contain cluster richness class, Bautz-Morgan type and distance class from the Abell (1958) and Leir - van den Bergh (1977) catalogs, and the last column contains the cluster contribution to the X-ray luminosity function which is discussed in Section IV. Table 2 lists the accompanying 90% error boxes for the clusters in Table 1. The 1950 right ascension and declination of the X-ray source are followed by the coordinates of the vertices of the error box, and the area of the error box in square degrees. Table 3 lists the best fit intensities and  $1\sigma$  errors for the non-detections in our sample. Our results are in agreement with those of Ricketts (1978) and Jones and Forman (1978) with the exception of Abell 576, A176 and A2657. For a discussion of A576 see Pravdo et al. 1979. We estimate that Table 1 is ~ 80% complete to 0.7 R15 counts per second; this is based on the observation that a source of this amplitude may be reduced to the confusion limit (0.5) with a resulting increase in  $\chi^2$  of 4 (corresponding to an 80% confidence interval).



#### IV. ANALYSIS

Prior to the HEAO experiments the most comprehensive list of X-ray sources associated with clusters of galaxies was the combined Second Ariel and Fourth Uhuru Catalog listings compiled by Jones and Forman (1977). This compilation is estimated by them to be complete to 2.5 Uhuru counts. The list of HEAO A-2 detections in Table 1 is estimated to be 80% complete to 0.7 R15 ( $\approx$  UFU), a factor of three improvement in sensitivity and thus represents a new basis for analysis of the relationships of X-ray luminosity, Bautz-Morgan class, and richness, and provides the data for an improved X-ray luminosity function of Abell clusters. It should be borne in mind that our search list of 225 clusters represents a statistically homogenous and complete sample of clusters. It is not a complete list of known clusters. Thus, if a cluster is not listed in Table 1, non-detection by HEAO-A2 is implied only if the cluster is an Abell cluster meeting Abell's statistical sample's galactic latitude and declination restrictions is of distance class four or less.

##### a. Luminosity and Bautz-Morgan Class

Figure 1 shows the relationship of X-ray luminosity and Bautz Morgan class for clusters in Table 1 which have fluxes greater than 0.7 R15. (A133 is not shown as it has not been classified in the BM system). There is a large amount of scatter in the diagram, but the median Type I luminosity is greater than that of Type III ( $9.4 \times 10^{44}$  erg s<sup>-1</sup> vs.  $3.1 \times 10^{44}$  erg s<sup>-1</sup>). Further, Figure 2 illustrates that Type I and I-II are more likely to be X-ray emitters than are later types. McHardy (1978) has suggested that within a given richness class, there might be a tighter relation between X-ray luminosity and BM type. In Figure 1 we have indicated clusters of richness class 2; the distribution with luminosity is not significantly different than that for all clusters. We have computed differential luminosity functions for BM classes I-(I-II), II-(II-III) and III, and fitted them with exponential forms, so that  $dN/dL$ , the differential luminosity function is approximated by  $Ke^{-L/L_0}$ , where  $L_0$  is the e-folding luminosity. The calculation of the luminosity function is discussed in detail below; here we wish only to compare

e-folding luminosities for the BM classes. These are tabulated in Table 4, along with 68% confidence brackets, corresponding to an increase in  $\chi^2$  of 2.1 as compared to the best-fit  $\chi^2$  (Lampton, Margon and Bowyer 1976). The e-folding luminosities increase smoothly from Type III to I and I-II, but the  $\chi^2$  test shows that there is only a 75.0% chance (corresponding to a  $\Delta\chi^2$  of 1.4) that the Type I-(I-II) e-folding luminosity is greater than that of Type III.

b. Rood-Sastry Type

Figure 3 is a plot of X-ray luminosity versus Rood-Sastry type (Rood and Sastry 1971). The plot includes only the sample clusters of distance class three or less that have been classified since the Rood-Sastry system does not extend to class four or include all class three clusters. In the past, Bahcall (1974) has stated that there is a correlation of X-ray luminosity with Rood-Sastry type, while more recently, Jones and Forman (1978) have claimed that this is simply a selection effect in that existing low luminosity cD clusters were below the sensitivity limits of Uhuru and Ariel. Our sample of distance class three (and closer) clusters contains 21 cD-B clusters, of which 11 were detected by A-2, and 33 ICF clusters, of which 10 were detected. There are only 3 L clusters in the sample, of which one was detected.

To answer the question as to whether or not there is a real difference between the cD-B luminosities and the ICF luminosities, we have calculated luminosity functions for each, and again fit the calculations with an exponential (Table 4). The fitted functions satisfy the constraints provided by the non-detections. The  $\chi^2$  test shows that there is a 95% chance (which corresponds to  $\Delta\chi^2$  of 4.6) that the cD-B e-folding luminosity is greater than the ICF e-folding luminosity. We also note that of 11 RS Type I clusters in the sample, the most luminous is  $1.3 \times 10^{44} \text{ erg s}^{-1}$  while of the cD-B clusters, 11 out of 21 exceed this luminosity. In view of this fact and the result of the luminosity function comparisons, we conclude that there is certainly a correlation of X-ray luminosity and Rood-Sastry type. This may of course be a by-product of the correlation between richness and luminosity, as most cD clusters are richness class 2 clusters as well. (Also noted by Jones and Forman 1978).

c. Luminosity and Richness

It has been pointed out by several authors (Jones and Forman 1978; deRoux and van den Berg 1977) that BM type is related to richness; that is Type I clusters are more often found among richness class 2 clusters than among 1 or 0. Any relationship between X-ray luminosity and BM type, or Rood-Sastry type may therefore simply be a by-product of the luminosity--richness relationship. The luminosity-richness relation is thus of fundamental importance. Abell (1958) defines richness class 2 as clusters containing from 80-129 galaxies no dimmer than 2 magnitudes than the third brightest cluster member, class 1 corresponds to 50-79, and class 0 from 30-49. Our sample contains 21 richness class 2 clusters, of which 11 were detected, 87 richness class 1's, of which 14 were detected, and 115 richness class 0 clusters, of which 7 were detected (Figure 5). Two richness class 3 clusters are also in the sample, neither of which were detected. In Figure 4 we have plotted X-ray luminosity versus Abell's richness class for our complete sample (flux > 0.7 R15). The results expressed in Figs. 4 and 5 conform to expectations based on the Second Ariel-Fourth Uhuru results and theories of X-ray emission. The median 2-10 keV luminosities of the detected clusters for richness classes 0, 1, and 2 are  $2.5 \times 10^{44}$  erg s<sup>-1</sup>,  $4.5 \times 10^{44}$  erg s<sup>-1</sup> and  $9.4 \times 10^{44}$  erg s<sup>-1</sup>, respectively. The luminosity function has been calculated and fitted by an exponential for each class, and the e-folding luminosities are listed in Table 4. There is only a 75.0% chance ( $\Delta\chi^2 = 1.4$ ) that the class 0 and class 1 luminosities are different, but there is a 95% ( $\Delta\chi^2 = 4.6$ ) chance that the class 2 luminosity is greater than that of class 0. The class 2 and class 1 e-folding luminosities can be said to be different with 84% confidence, or  $\Delta\chi^2 = 3.2$ .

d. Luminosity Function

As well as providing the number density of clusters of a given X-ray luminosity, the luminosity function is of interest in that it provides the average cluster luminosity and an estimate of the contribution of X-ray clusters to the diffuse X-ray background. Prior to the HEAO-1 mission the best available X-ray luminosity functions have been those of McHardy (1978) and Schwartz (1978) which are based on the Second Ariel and Fourth Uhuru Catalogs. Schwartz, using the Uhuru data base, has drawn on the same sample of Abell clusters as our own, and computed the luminosity function for clusters in distance class less than or equal to three and brighter than 2.5 UFU, of which there are 6. McHardy has employed the Ariel 5 data, but has not limited himself to a statistically complete sample; there are 20 X-ray clusters in his sample brighter than his survey limit of 0.6 Ariel counts per sec ( $\sim 1.5$  UFU). The present survey has been designed expressly for the purpose of re-calculating the luminosity function, using as a basis one which is as large and unbiased as possible. The greater sensitivity of the A2 detectors, as compared to the Uhuru and Ariel experiments, makes it possible to reliably extend the luminosity function to distance class four. As a result of the A2 detections, there are now 30 sources identified as clusters brighter than 0.7 R15 in the statistical sample ( $D \leq 4$ ) available for calculation of a luminosity function, as compared to 15 well known sources.

Table 5 lists the calculated values of the differential luminosity function  $dN/dL$ , and Figure 6 is a graph of this function. Only clusters brighter than or equal to 0.7 R15 are included as this is the completeness limit. The clusters have been binned in intervals in  $L_{44}$  containing three clusters each and the volume density in each bin has been divided by the luminosity range of the bin so that the units of the luminosity function  $f(L)$ , are  $\text{Mpc}^{-3}$  per  $10^{44}$  erg  $\text{s}^{-1}$  per 2-10 keV. The contribution of each cluster to the luminosity function has been calculated by the maximum volume method, i.e. the distance to which a given cluster could be removed and still be brighter than 0.7 R15 has computed along with the corresponding volume. This volume is not allowed to exceed the sample

volume, which is limited to  $z < 0.1$ . The maximum distance of detection and volume has been computed to first order in  $z$ ; that is,  $\text{volume} = (cz/H)^3$ . This is exactly true for  $q = 1$ , and introduces a maximum error of 15% if  $z = 0.1$  and  $q = 0$ . Even if  $q = 0$ , however, the error is negligible ( $< 1\%$ ) for  $z < 0.05$ . The test for an unbiased sample is that the average value of  $V/V_{\text{max}}$  should be 0.5; for our cluster sample this average is  $0.55 \pm 0.10$ . The standard deviations listed in Table 5 were calculated via Felten's (1976) formula (Equation 18).

We have found that the luminosity function can be well represented analytically by either an exponential or a power law between  $0.5 \times 10^{44}$  and  $2.0 \times 10^{45}$  erg s $^{-1}$ , which is the interval for which we have an acceptable number of representative clusters. Analytic fits must meet two boundary conditions: (1) the integral of  $f(L)$  over all luminosities must be less than the total volume density of clusters in the survey, and (2) the total number of sources of all luminosities must be less than that predicted by the  $\log N - \log S$  curve. Exponential fits are generally well-behaved and do not violate these boundary conditions, while power law fits must be truncated to fit the constraints. For an exponential of the form  $f(L) = Ke^{-L/L_0}$ , our calculated function is fit by  $K = 20.2 \times 10^{-8}$  Mpc $^{-3}$  per  $10^{44}$  erg s $^{-1}$ , and  $L_0 = 1.9 \times 10^{44}$  erg s $^{-1}$  (2-10 keV). Upper limit data were not used in this calculation. The reduced  $\chi^2$  for the exponential fit is 0.92 per degree of freedom, and the 68% (1 $\sigma$ ) combined confidence intervals for  $K$  and the e-folding luminosity are  $32.2$  to  $10.2 \times 10^{-8}$  Mpc $^{-3}$  per  $10^{44}$  erg s $^{-1}$  and  $1.5$  to  $2.5 \times 10^{44}$  erg s $^{-1}$ , respectively (Fig. 7). This representation can be extrapolated to zero and finity without violation of the boundary conditions. The integral over all luminosities is

$$\int_0^\infty Ke^{-L/L_0} dL = 0.39 \times 10^{-6} \text{ Mpc}^{-3},$$

which is 40% of the total sample cluster density,  $0.95 \times 10^{-6}$  Mpc $^{-3}$ . The number of clusters per steradian in the sample volume brighter than 0.7 R15 predicted by the exponential is

$$3.8 \times 10^6 \int_0^\infty L_{44}^{3/2} f(L) dL_{44} = 5.0 \text{ sr}^{-1}.$$

The A-2 log N - log S curve predicts 21 per steradian, so approximately 25% of all high galactic latitude X-ray sources may be expected to be clusters with  $kT > 2 \text{ keV}$ .

The observed luminosity function may also be modeled as a power law. If  $f(L) = KL_{44}^{-\alpha}$ , then a reduced  $\chi^2$  of 0.97 per degree of freedom is obtained for  $K = 23.3 \times 10^{-8} \text{ Mpc}^{-3} \text{ per } 10^{44} \text{ erg s}^{-1}$  and  $\alpha = 2.03$ . The 68% combined confidence brackets for K and  $\alpha$  are  $11.0 \times 10^{-8}$  to  $35.3 \times 10^{-8} \text{ Mpc}^{-3} \text{ per } 10^{44} \text{ erg s}^{-1}$  and 1.7 to 2.3 respectively. The power law cannot be extrapolated to zero and infinite luminosity as the boundary conditions are violated. Between  $0.5 \times 10^{44}$  and  $2.0 \times 10^{45} \text{ erg s}^{-1}$ , however, the constraints are satisfied; the integral of f over the luminosities in this interval is  $3.5 \times 10^{-7} \text{ Mpc}^{-3}$  and the number of sources predicted in this range is 6.7 per steradian<sup>1</sup>.

<sup>1</sup>During the course of this work, spectroscopic redshifts for our entire sample were obtained by Hintzen, Scott and McKee (1980). These redshifts change our values for K and  $L_0$  by about 20%. See the paper that follows for details.

Given an analytic representation of  $f(L)$  one can then ask what the cluster contribution to the X-ray background is. This contribution may be considered in two ways. The first is to simply calculate the integrated volume emissivity for the cluster luminosity function and compare it to the X-ray background volume emissivity. We shall use the exponential representation of  $f(L)$  for this purpose as the power law result is sensitive to the range of luminosities within which it is considered valid. The cluster integrated volume emissivity is thus

$$\int_0^\infty L f(L) dL = 7.3 \times 10^{37} \text{ erg s}^{-1} \text{ Mpc}^{-3} \text{ per 2-10 keV.}$$

The volume emissivity of the X-ray background depends upon various factors discussed by Schwartz and Gursky (1975). For a universe in which  $q_0$  is  $\frac{1}{2}$ , the Hubble constant is 50 km/sec/Mpc, and  $z_{\text{max}} = 3$ , the 2-10 keV background volume

emissivity is  $1.5 \times 10^{39} \text{ erg s}^{-1} \text{ Mpc}^{-3}$  and the cluster volume emissivity is 4.9% of this figure. The error in the cluster contribution is less than would be indicated by the error in the luminosity function parameters as these parameters and errors are highly correlated:  $\chi^2$  tests give a 90% confidence bracket of  $\pm 8\%$  for the percentage of X-ray background due to the clusters (Fig. 7). Volume emissivities are not the most informative comparison of background and clusters, however, because the two have widely different spectra. This brings us to the second, preferable method of expressing the cluster contribution, namely comparing background and cluster intensities at given energies. To convert the cluster luminosity function and volume emissivity to intensities it is necessary to obtain  $B(E)$ , the emissivity per keV. If we use the typical cluster spectrum (Mushotzky et al. 1978), and require that the integral of  $B(E)$  over 2-10 keV equal the cluster volume emissivity calculated above, we find  $B(E) = 4.2 \times 10^{37} E^{-0.4} e^{-E/6} \text{ erg s}^{-1} \text{ Mpc}^{-3} \text{ keV}^{-1}$ . The intensity is related to  $B(E)$  by  $I(E) = 1/4\pi \cdot C/H_0 \cdot B(E) \cdot J(q_0, Z_{\text{max}}, E)$ , where  $J$  is a spectrally dependent integral discussed by Avni (1978). For  $q_0 = \frac{1}{2}$  and  $Z_{\text{max}} = 3$ ,  $J$  is 0.35 at 4 keV and 0.25 at 10 keV, the X-ray intensity at 4 and 10 keV is thus 0.15 and 0.038 keV/(keV sec  $\text{cm}^2 \text{ sr}$ ) respectively. The X-ray background at 4 and 10 keV is  $\sim 4.8$  and 3.2 keV/(keV sec  $\text{cm}^2 \text{ sr}$ ) (Marshall et al. 1980), so the percentage of the total X-ray background contributed by clusters at 4 keV is 3.1% and 10 keV is 1.2%. When one allows for the fact that cluster luminosities are uncertain to  $\sim 20\%$  because of the uncertainty in cluster temperatures, and for the fact that the survey is only  $\sim 80\%$  complete, and adds these uncertainties to the statistical error in  $f(L)$ , the maximum contribution at 4 and 10 keV is still less than 5% and 3% respectively, at 90% confidence. If the true value of the cluster contribution is indeed 1-5%, as found here, it would alleviate a problem found by Marshall et al. (1980) in modelling the X-ray background. Those authors found that thermal bremsstrahlung from a gas with  $kT = 40 \text{ keV}$  fit the observed background spectrum well, provided that a large cluster contribution was not subtracted. Cluster

contributions as high as 20 or 30%, such as implied by previous luminosity functions (e.g. Schwartz 1978), would make a thermal fit to the background in the 2-10 keV band difficult. (Schwartz's (1978) data and results are not in conflict with our own, however, when his luminosity function is re-calculated using the revised 4U fluxes for clusters (Jones and Forman 1978)).

Figures 8a and b compare the present luminosity function data with the 4U and 2A data base used by Schwartz (1978) and McHardy (1978) respectively. The data have been presented as integral luminosity functions, i.e. the sum of all cluster contributions corresponding to clusters brighter than a given luminosity. This integral, or sum, has been computed for luminosities corresponding to all the individual cluster luminosities, consequently each sequential point in Figure 8 represents one less cluster in the sum than the one before it, and the difference between the points is the value of the differential luminosity function in that range of  $L$ . Schwartz and McHardy's data have been re-computed in the same manner as our data, that is we have converted their luminosities to 2-10 keV luminosities (using  $kT = 7$  keV) and limited Schwartz's maximum volumes to  $z = 0.07$  since his complete sample includes only distance class three clusters, or closer, and limited McHardy's maximum volumes to  $z = 0.1$ . McHardy's sample is not statistical nor optically complete, so the maximum volume allowable would be undefined, but beyond  $z = 0.1$ , most Abell clusters would not be recognized as X-ray clusters and so would not be in the sample volume. Given these modifications, Schwartz and McHardy's data are in agreement with our own (Figure 8). Without these modifications, these data disagree with ours above  $10^{45}$  erg s $^{-1}$ , where they predict 3x fewer clusters than we have actually seen.



Given the present constraints and capabilities of the A-2 experiment we are confident that the luminosity function is now well determined between  $5 \times 10^{43}$  erg s<sup>-1</sup> and  $10^{45}$  erg s<sup>-1</sup>. Beyond either of these limits, however, we cannot be sure that the luminosity function is well represented by the analytic functions discussed. In particular, for clusters with luminosities below  $\sim 5 \times 10^{43}$  erg s<sup>-1</sup>, we expect that the cluster temperatures will fall well below the 'typical' cluster temperature of 7 keV assumed in order to calculate the luminosity. Clusters with temperatures  $\lesssim 3$  keV require a large correction in calculating the absolute flux and are also unlikely to be detected by A-2 since the instrument sensitivity falls off sharply below 2-3 keV. As to effect of this on the cluster contribution to the X-ray background, the maximum possible value of the cluster contribution is obtained if one extrapolates a power law fit made to the five least luminous clusters in our sample down to the luminosity at which the integral luminosity function (Fig. 7b) equals the space density of all Abell clusters. This luminosity is  $2 \pm 2 \times 10^{43}$  erg s<sup>-1</sup>. Below this luminosity, the most drastic assumption one can make is that all the remaining Abell clusters have this X-ray luminosity. The maximum possible value (90% confidence) of the volume emissivity thus obtained is then 8% of the X-ray background. This is consistent with the upper limit of 7% which McHardy (McHardy, private communication; Warwick 1979) has obtained from the 2A data base, once it was corrected for confusion noise and non-uniform sky coverage.

## V. SUMMARY

We have examined a statistically complete sample of 225 Abell clusters and have found

1. twelve new identifications of clusters with X-ray sources,
2. that  $L_x$  is roughly correlated with richness for richness classes 0, 1 and 2,
3. that  $L_x$  is well-correlated with Rood-Sastry type and only loosely correlated with Bautz-Morgan type, and

4. that the luminosity function has been over-estimated in the past and that the cluster contribution to the X-ray background is  $\lesssim 5\%$  between 2 and 10 keV.

The present survey and luminosity function is the best that can be done with the existing optical catalog and the HEAO A-2 data. Increased sensitivity in the X-ray regime, such as represented by HEAO-2, will help in determining the luminosity function, but there will be severe optical completeness problems and the large kT correction which will be unknown for the low temperature, low luminosity clusters discovered by HEAO-2. In a subsequent paper, we will present kT's for the clusters in this paper. Beyond this, southern catalogs of clusters must be completed before further progress can be made with the A-2 experiment.

#### VI. ACKNOWLEDGMENTS

This work was supported by NASA grant NAS8-33346.

## REFERENCES

- Abell, G. 1958, Ap. J. Supplement 3, 211.
- Avni, Y. 1976, Astron. and Astrophys. 63, L13.
- Bahcall, N. 1978, Ap. J. (Letters) 224, L7.
- Felten, J.E. 1976, Ap. J. 207, 700.
- Gursky, H., Kellogg, E., Murray, S., Leong, C., Tananbaum, H., and  
Giacconi, R. 1971, Ap. J. (Letters) 167, L81.
- Gursky, H., Solinger, A., Kellogg, E., Murray, S., Tananbaum, H.,  
Giacconi, R., and Cavalierie, A. 1972, Ap. J. (Letters) 173, L99.
- Hintzen, P. and Scott, J.S. 1977, Ap. J. 212, 8.
- Jones, C. and Forman W. 1978, Ap. J. 224, 1.
- Lampton, M., Margon, B., and Bowyer, S. 1976, Ap. J. 208, 177.
- Leir, A. and van den Bergh, S. 1977, Ap. J. Supplement 34, 381.
- Marshall, F.E., Boldt, E.A., Holt, S.S., Mushotzky, R.F., Pravdo, S.H.,  
Rothschild, R., and Serlemitsos, P.J. 1979, Ap. J. Supplement  
Marshall, F.E., Boldt, E.A., Holt, S.S., Miller, R., Mushotzky, R.F., Rose, L.A.,  
Rothschild, R., and Serlemitsos, P. 1980, Ap. J., in press.
- McHardy, I. 1978, M.N.R.A.S. 182, 760.
- Mitchell, R.J., Culhane, J.L., Davison, P.J.N., and Ives, J.C. 1976,  
M.N.R.A.S. 176, 29P.
- Mushotzky, R.F., Serlemitsos, P.J., Smith, B.W., Boldt, E.A., and Holt, S.S.  
1978, Ap. J. 225, 21.
- Pravdo, S.H., Boldt, E.A., Marshall, F.E., McKee, J.D., Mushotzky, R.F., and  
Smith, B.W. 1979, Ap. J., in press.
- Ricketts, M.J. 1978, M.N.R.A.S. 183, 51p.
- Rood, H.J. and Sastry, G.N. 1971, P.A.S.P. 83, 313.
- Rothschild, R., Boldt, E., Holt, S., Serlemitsos, P., Garmire, G., Bowyer, S.,  
and Lampton, M. 1979, Space Sci. Instrumentation 4, 269.
- Schwartz, D. 1978, Ap. J. 220, 8.

Schwartz, D. and Gursky, H. 1975, X-Ray Astronomy, R. Giacconi, ed., D. Reidel Co., Boston, p. 359.

van den Bergh, S. and de Roux, J. 1978, Ap. J. 219, 352.

Vidal, N.V. and Peterson, B.A. 1975, Ap. J. (Letters) 196, L95.

Warwick, R. 1979, Proc. of the Royal Soc. of London, 366A, 391.

## TABLE CAPTIONS

- Table 1 - Clusters of galaxies detected as X-ray sources. Fluxes are in R15 units ( $\approx 1$  UFU). Intensities do not include confusion noise, but or fluxes greater than 1.0, this is a very small error.
- Table 2 - 90% error boxes for detections.
- Table 3 - Upper limits for non-detections with  $1\sigma$  errors. For some sources distance of emission centroid from cluster is given in degrees.
- Table 4 - 2-10 keV e-folding luminosities vs. Bautz-Morgan type, Rood-Sastry type and Abell richness class. The upper and lower limits are for 68% confidence.
- Table 5 - Differential X-ray luminosity function. Luminosities are 2-10 keV in units of  $10^{44}$  erg sec $^{-1}$ .  $\bar{L}_x$  is the average luminosity for the bin,  $f(L)$  is the computed luminosity function,  $\sigma$  is the standard deviation (Felten 1976) and the number of clusters in the bin is listed along with exponential fit to  $f(L)$ .

TABLE 1

NAME	FLUX	L <sub>44</sub>	Z	REF. <sup>1</sup>	R	BM	D	$V_m^{-1} \times 10^{-8} \text{ Mpc}^{-3}$
A85	$2.64 \pm 0.24$	6.7	0.050		1	I	4	0.351
A119	$1.74 \pm 0.33$	3.7	0.045		1	II-III	3	0.836
A133	$0.83 \pm 0.23$	4.6	0.072		0		4	.619
A151	$1.16 \pm 0.14$	6.1	0.069		1	II:	3	0.426
A195	$0.90 \pm 0.28$	1.8	0.0436	N	0	I-II	3	2.47
A401	$2.95 \pm 0.24$	17.4	0.075	HS	2	I	3	$0.298^2$
A496	$1.77 \pm 0.25$	2.64	0.036	LV	1	I:	3	1.42
A993	$0.70 \pm 0.18$	1.3	0.042		0	III	3	3.96
A1225	$0.68 \pm 0.20$	2.3	0.056		0	III	3	----
A1254 *	$0.87 \pm 0.10$	2.2	0.049		1	III	3	1.80
A1314 *	$0.74 \pm 0.21$	0.50	0.025		0	III	1	16.6
A1367	$1.14 \pm 0.14$	0.49	0.0205	LV	2	II-III:	1	17.4
A1382 *	$0.79 \pm 0.14$	5.7	0.082		1	II:	4	0.452
A1474 *	$0.97 \pm 0.15$	6.8	0.081		1	III	4	0.342
A1644 *	$1.45 \pm 0.28$	5.8	0.061		1	II	4	0.439
A1651 *	$1.08 \pm 0.26$	6.4	0.074		1	I-II	4	0.381
A1656	$14.67 \pm 0.28$	8.47	0.0230	LV	2	II	1	0.298
A1767	$0.51 \pm 0.16$	2.6	0.069		1	II	4	----

A1795	$2.36 \pm 0.25$	10.1	0.0630	LV	2	I	4	0.298
A1904	$0.70 \pm 0.20$	3.9	0.0719	LV	2	II-III:	3	0.797
A2029	$3.00 \pm 0.29$	19.5	0.0777	LV	2	I	4	0.298
A2052	$1.51 \pm 0.28$	3.9	0.049		0	I-II	3	$0.805^3$
A2061	$0.90 \pm 0.14$	4.5	0.068		1	III:	4	$0.656^4$
A2065	$1.00 \pm 0.14$	5.6	0.0722	LV	2	III	3	0.473
A2124	$0.87 \pm 0.24$	3.3	0.059		1	I	3	1.04
A2142	$3.14 \pm 0.23$	16.1	0.069		2	II	4	$0.298^5$
A2147	$1.82 \pm 0.23$	2.73	0.0377	LV	1	III	1	1.37
A2199	$2.72 \pm 0.18$	2.80	0.0312	LV	2	I	1	$1.28^5$
A2255	$0.65 \pm 0.10$	2.7	0.062		2	II-III:	3	----- 6,7
A2256	$2.53 \pm 0.18$	8.2	0.055		2	II-III:	3	0.298
A2440	$0.83 \pm 0.25$	2.86	0.0567	LV	0	II	4	1.28
A2657	$1.31 \pm 0.27$	2.37	0.0414	LV	1	III	3	1.63

<sup>1</sup>LV = Leir and van den Bergh, 1977; HS = Hintzen and Scott, 1978; N = Noonan, 1973; V = Vidal and Peterson, 1975.  
Where reference is not given, redshift is from apparent magnitude of  $10^{11}$  brightest galaxy

(Leir and van den Bergh 1977; Rowan-Robinson 1972).

<sup>2</sup>The centroid of the X-ray emission from A401 and A399 lies between the two clusters, but the emission is satisfactorily modeled with point sources at A401 and A399. The flux from A399 is  $< 2.5$  counts per sec.

<sup>3</sup>Confused with A2040 in scan angle.

<sup>4</sup>A2061 and 2067 both lie within X-ray error box but best position is on A2061

5 possibly extended  $\sim 1^0$  or confused with unknown source.

6 No evidence for extent or confusion.

7 Not included in luminosity function because  $I < 0.7$

\* New detections



TABLE 2. 1950 RA/DEC

(1)	(2)	(3)	(4)	(5)	(6)	(7)	(8)	(9)	(10)	(11)	(12)
A85	009.54	-009.75	009.80	-009.40	008.90	-009.95	009.06	-010.35	009.99	-009.85	0.47
A119	013.40	-001.70	014.00	-001.22	013.06	-001.64	013.25	-002.10	014.17	-001.70	0.50
A133	015.60	-022.50	014.80	-023.04	016.87	-022.15	016.05	-021.45	014.50	-022.36	1.6
A151	017.56	-015.53	015.81	-015.50	018.22	-014.40	018.84	-015.80	016.37	-016.85	3.2
A195	021.74	19.00	20.45	18.84	22.54	19.70	22.83	18.77	20.74	18.02	1.8
A401	043.88	013.25	044.43	013.59	043.53	013.34	043.67	012.96	044.53	013.21	0.33
A496	068.68	-013.10	070.68	-012.20	067.73	-012.91	067.88	-014.75	070.88	-013.00	2.77
A993	157.2	-005.60	154.60	-003.69	154.00	-005.07	157.54	-006.55	158.15	-005.20	5.5
A1225	171.86	53.14	169.00	54.75	173.56	52.91	173.25	52.13	168.15	53.97	2.5
A1254	170.53	071.46	172.00	071.13	169.20	072.19	168.66	070.81	171.44	069.78	1.42
A1314	173.33	049.58	174.67	049.78	172.57	050.56	172.12	049.43	174.22	048.63	1.75
A1367	175.83	020.19	176.39	020.25	175.46	020.65	175.22	020.07	176.14	019.71	0.56
A1382	175.44	071.38	176.82	071.20	174.71	072.55	174.26	071.23	176.28	070.59	1.12
A1474	182.00	015.33	182.92	015.55	181.45	016.21	180.90	015.05	182.43	014.39	1.60
A1644	193.74	-016.92	194.64	-016.91	193.68	-016.54	193.42	-017.14	194.37	-017.51	0.65
A1651	194.44	-004.25	195.54	-004.10	193.26	-003.34	193.00	-003.95	194.79	-004.75	1.37
A1656	194.17	028.15	194.36	028.15	194.08	028.27	194.02	028.16	194.30	028.04	0.026
A1767	202.35	59.41	201.30	60.97	204.45	59.02	203.80	58.07	200.50	59.82	2.80
A1795	206.66	026.89	207.13	026.94	206.28	27.32	206.06	26.86	206.92	26.48	0.43
A1904	217.51	047.60	218.05	047.52	215.10	048.77	214.95	048.67	217.90	047.22	0.40
A2029	226.91	006.00	227.71	006.03	226.32	006.45	226.21	006.02	227.33	005.60	0.56

A2052	228.36	007.09	227.60	007.79	227.34	006.93	229.13	006.40	229.39	007.26	1.62
A2061	229.91	30.81	231.21	031.05	229.01	31.80	228.63	30.83	230.82	30.02	2.25
A2065	229.51	028.90	230.61	28.43	228.64	29.15	228.24	28.32	230.33	27.67	1.37
A2108	234.68	017.98	236.65	017.40	233.05	019.00	232.75	017.55	236.35	016.45	4.7
A2124	236.61	035.92	238.29	035.63	235.76	036.49	235.56	035.99	238.09	035.13	1.20
A2142	238.21	27.54	240.22	027.15	237.97	027.82	237.82	027.43	240.11	026.78	0.84
A2147	240.68	16.03	241.74	016.87	239.72	017.29	239.37	016.00	241.34	015.01	3.63
A2199	247.26	39.58	248.56	039.36	246.11	039.96	246.01	039.71	248.46	39.06	0.81
A2255	257.72	064.41	258.46	064.54	257.62	065.04	257.09	064.34	257.88	63.72	0.65
A2256	256.59	078.66	257.68	078.89	255.63	078.74	255.68	078.47	257.73	078.64	0.10
A2440	335.80	-001.69	336.90	-000.61	334.46	-001.63	334.93	-002.74	337.38	-001.76	3.24
A2657	335.90	009.00	356.96	009.85	355.10	009.12	355.43	008.30	357.30	009.07	1.72

TABLE 3. UPPER LIMITS

	FLUX	DEG.		FLUX	DEG.		FLUX	DEG. <sup>1</sup>
A14	0.3 ± 0.20		A189	0.24 ± 0.25		A634	0.00 ± 0.21	
A21	0.35 ± 0.29		A193	0.90 ± 0.30	0.7	A671	0.00 ± 0.14	
A43	0.33 ± 0.29		A194	0.00 ± 0.08		A692	0.67 ± 0.18	1.6
A71	0.37 ± 0.27		A225	0.00 ± 0.15		A757	0.10 ± 0.16	
A74	0.52 ± 0.27		A240	0.00 ± 0.16		A762	0.00 ± 0.18	
A76	0.00 ± 0.15		A245	0.67 ± 0.27		A779	0.00 ± 0.20	
A86	0.00 ± 0.25		A246	0.36 ± 0.24		A786	0.38 ± 0.17	
A88	0.00 ± 0.16		A260	0.30 ± 0.21		A787	0.27 ± 0.12	
A102	0.39 ± 0.26		A274	0.21 ± 0.24		A834	0.93 ± 0.10	3.2
A103	0.54 ± 0.21	0.6	A277	0.11 ± 0.24		A912	0.69 ± 0.28	
A114	0.34 ± 0.46		A309	0.38 ± 0.21		A933	0.00 ± 0.06	
A116	0.62 ± 0.29		A397	0.00 ± 0.15		A957	0.05 ± 0.21	
A117	0.65 ± 0.26		A399	2.50 ± 1.12		A978	0.10 ± 0.21	
A121	0.00 ± 0.14		A400	0.45 ± 0.24		A999	0.55 ± 0.15	1.2
A134	0.60 ± 0.26		A415	0.22 ± 0.24		A1016	0.00 ± 0.26	
A147	0.17 ± 0.23		A500	0.00 ± 0.18		A1020	0.00 ± 0.20	
A154	0.00 ± 0.10		A514	0.35 ± 0.14		A1032	0.20 ± 0.20	
A158	0.00 ± 0.27		A564	0.00 ± 0.17		A1035	0.41 ± 0.18	0.2
A160	0.00 ± 0.24		A568	0.21 ± 0.18		A1069	0.00 ± 0.25	
A168	0.38 ± 0.22		A576	0.54 ± 0.14	1.6	A1097	0.61 ± 0.20	
A171	0.00 ± 0.28		A595	0.56 ± 0.18	3.0	A1100	0.10 ± 0.21	
A179	0.38 ± 0.26		A628	0.24 ± 0.17		A1126	0.55 ± 0.20	0.5

A1139	0.21 ± 0.21	A1364	0.00 ± 0.20	A1783	0.37 ± 0.17
A1142	0.38 ± 0.19	A1365	0.42 ± 0.17	A1793	0.28 ± 0.20
A1145	0.24 ± 0.23	A1377	0.14 ± 0.23	A1800	0.40 ± 0.14
A1149	0.00 ± 0.18	A1383	0.00 ± 0.20	A1809	0.35 ± 0.23
A1171	0.40 ± 0.25	A1390	0.00 ± 0.20	A1813	0.46 ± 0.18
A1177	0.27 ± 0.20	A1399	0.71 ± 0.20	A1825	0.61 ± 0.16
A1185	0.45 ± 0.20	A1412	0.67 ± 0.14	A1831	0.10 ± 0.21
A1187	0.27 ± 0.18	A1436	0.63 ± 0.19	A1836	0.34 ± 0.28
A1213	0.00 ± 0.20	A1452	0.46 ± 0.21	A1837	0.48 ± 0.21
A1216	0.35 ± 0.17	A1465	0.57 ± 0.14	A1873	1.3 ± 0.21
A1218	0.51 ± 0.14	A1496	0.66 ± 0.21	A1890	0.51 ± 0.22
A1128	0.41 ± 0.18	A1500	0.00 ± 0.08	A1899	0.00 ± 0.25
A1238	0.15 ± 0.20	A1507	0.70 ± 0.15	A1913	0.30 ± 0.20
A1257	0.37 ± 0.24	A1541	0.20 ± 0.21	A1927	0.90 ± 0.22
A1270	0.31 ± 0.20	A1516	0.00 ± 0.22	A1983	0.00 ± 0.19
A1275	0.38 ± 0.18	A1631	0.67 ± 0.23	A1991	0.00 ± 0.19
A1291	0.51 ± 0.14	A1638	0.00 ± 0.15	A1999	0.25 ± 0.14
A1297	0.35 ± 0.17	A1691	0.76 ± 0.20	A2005	0.31 ± 0.20
A1308	0.39 ± 0.20	A1709	0.00 ± 0.26	A2019	0.00 ± 0.29
A1318	0.26 ± 0.20	A1749	0.56 ± 0.23	A2020	0.00 ± 0.30
A1332	0.25 ± 0.25	A1750	0.32 ± 0.20	A2022	0.00 ± 0.19
A1334	0.00 ± 0.25	A1773	0.20 ± 0.21	A2028	0.00 ± 0.21
A1336	0.45 ± 0.18	A1775	1.86 ± 0.16	A2033	0.00 ± 0.30
A1362	0.00 ± 0.25	A1781	0.68 ± 0.21	A2036	0.00 ± 0.21

A2040	1.6 ± 0.21	0.1 <sup>2</sup>	A2241	0.00 ± 0.35	A2462	0.00 ± 0.19
A2048	0.00 ± 0.30		A2247	0.13 ± 0.13	A2572	0.00 ± 0.20
A2055	1.22 ± 0.28		A2248	0.42 ± 0.19	A2589	0.52 ± 0.30
A2063	1.2 ± 0.80		A2271	0.30 ± 0.24	A2593	0.00 ± 0.20
A2067	0.90 ± 0.30	0.1 <sup>2</sup>	A2295	0.67 ± 0.13	A2618	0.37 ± 0.25
A2079	0.16 ± 0.20		A2301	0.46 ± 0.30	A2622	0.68 ± 0.20
A2089	0.60 ± 0.22		A2308	0.30 ± 0.20	A2625	0.65 ± 0.24
A2092	0.00 ± 0.30		A2309	0.00 ± 0.20	A2626	0.00 ± 0.23
A2107	0.00 ± 0.20		A2311	0.17 ± 0.10	A2630	0.26 ± 0.30
A2108	0.68 ± 0.40		A2347	0.20 ± 0.21	A2656	0.60 ± 0.30
A2148	1.04 ± 0.27		A2366	0.60 ± 0.26	A2660	0.00 ± 0.30
A2149	0.37 ± 0.15		A2382	0.49 ± 0.25	A2665	0.46 ± 0.30
A2151	1.10 ± 0.25	0.1 <sup>3</sup>	A2384	0.34 ± 0.17	A2670	0.00 ± 0.21
A2152	2.00 ± 0.25	0.1 <sup>3</sup>	A2399	0.41 ± 0.19	A2675	0.44 ± 0.22
A2159	0.73 ± 0.29		A2410	0.00 ± 0.10	A2700	0.30 ± 0.21
A2162	0.00 ± 0.24		A2412	0.30 ± 0.26		
A2169	0.00 ± 0.20		A2415	0.39 ± 0.20		
A2175	0.10 ± 0.21		A2448	0.00 ± 0.18		
A2184	0.38 ± 0.13		A2457	0.30 ± 0.26		
A2197	0.20 ± 0.20		A2459	0.20 ± 0.18		

<sup>1</sup>Deg is offset is the best fit position from the optical position of cluster

<sup>2</sup>See Table 1

<sup>3</sup>Source identified with A2147 (see Pravdo et al. 1979)

TABLE 4

<u>BAUTZ - MORGAN TYPE</u>	<u><math>L_0 \times 10^{44} \text{ erg s}^{-1}</math></u>	<u>LOWER LIMIT</u>	<u>UPPER LIMIT</u>
I - (I - II)	9.0	5.0	30.0
II - (II - III)	6.0	2.5	31.0
III	4.0	2.1	14.0
<u>ROOD - SASTRY TYPE</u>			
CD - B	3.9	3.4	----
I - C - F	1.6	1.0	4.0
<u>ABELL RICHNESS CLASS</u>			
2	14.0	5.5	----
1	4.5	2.0	10.0
0	2.6	0.3	12.0

TABLE 5

$\Delta L$	$\bar{L}$	$\Sigma V_m^{-1}/\Delta L$	$\sigma$
$10^{44} \text{ erg s}^{-1}$	$10^{44} \text{ erg s}^{-1}$	$10^{-8} \text{ Mpc}^{-3} \text{ per } 10^{44} \text{ erg s}^{-1}$	$10^{-8} \text{ Mpc}^{-3} \text{ per } 10^{44} \text{ erg s}^{-1}$
0.5 - 0.9	0.5	82.	59.
0.9 - 2.3	1.8	5.9	3.4
2.3 - 2.8	2.6	9.5	5.5
2.6 - 3.5	3.0	4.9	2.8
3.5 - 4.3	3.8	3.0	1.8
4.3 - 5.6	4.9	1.3	0.74
5.6 - 6.2	5.9	2.2	1.3
6.2 - 7.5	6.6	0.86	0.50
7.5 - 13.1	8.9	0.16	0.092
13.1 - 19.5	17.7	0.14	0.081

# APPENDIX

In the course of the cluster survey, all clusters in the Leir-van den Bergh catalog of distance class  $\leq 4$  were investigated. Six of these clusters were detected but are not in Abell's (1958) statistically complete survey space, and thus were not included in our sample on Tables 1 or 2. The fluxes and error boxes for these clusters are tabulated below in Tables 1A and 2A.

TABLE 1A

<u>NAME</u>	<u>FLUX</u>	<u>L<sub>44</sub></u>	<u>z</u>	<u>Ref.</u> <sup>1</sup>	<u>R</u>	<u>BM</u>	<u>D</u>
A262	0.32 $\pm$ 0.23	0.38	0.017	LV	0	III	1
A592	0.57 $\pm$ 0.23	1.7	0.052		1	I:	3
A644	1.26 $\pm$ 0.22	9.9	0.084		0	III:	4
A754	3.96 $\pm$ 0.28	10.4	0.052	LV	2	I-II:	3
A2319	6.10 $\pm$ 0.17	12.7	0.044	LV	1	II-III	3
A2666	1.06 $\pm$ 0.20	0.85	0.0273	V	0	III	1

<sup>1</sup>See Table 1 for redshift references

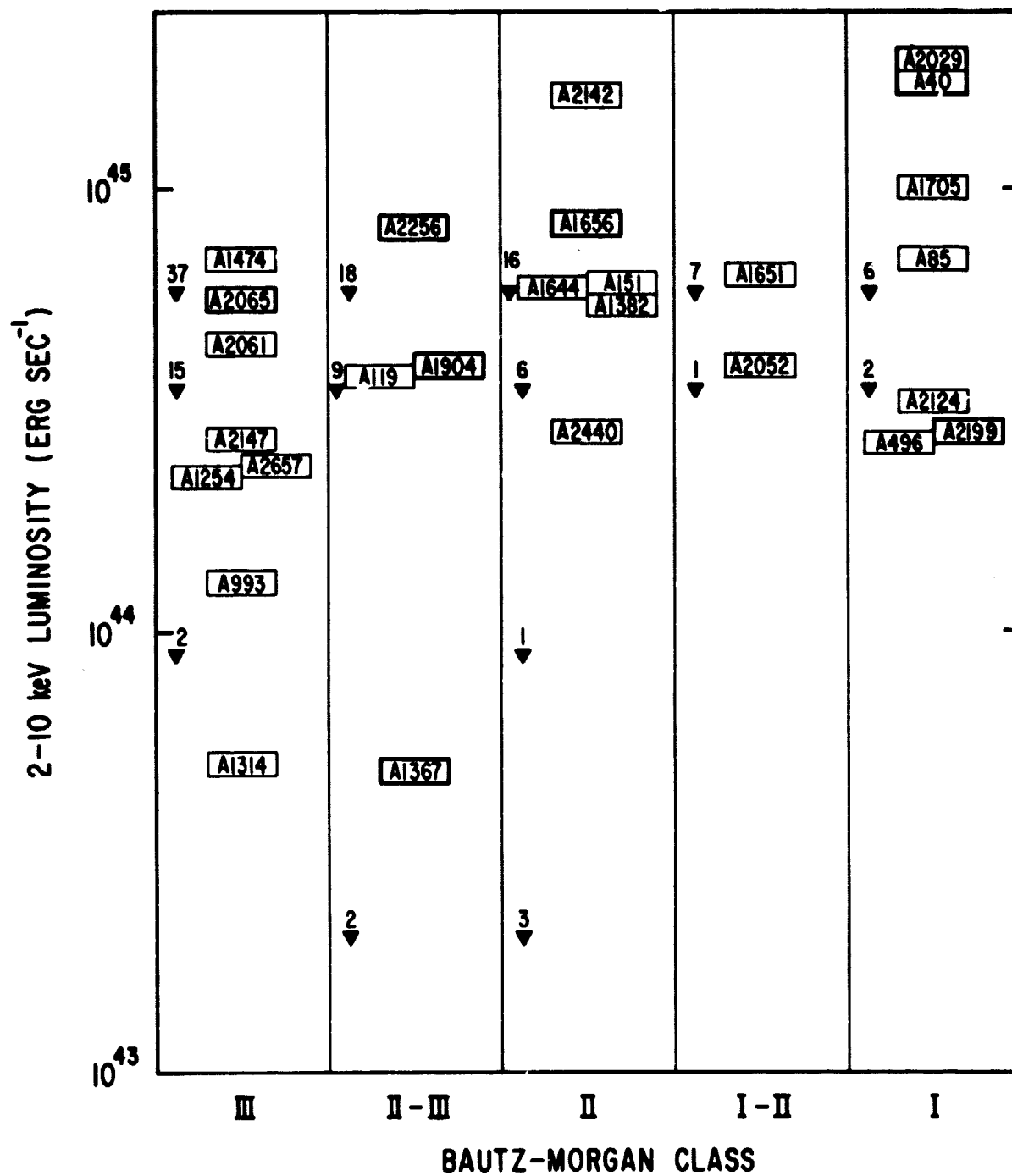
TABLE 2A 1950 RA/DEC

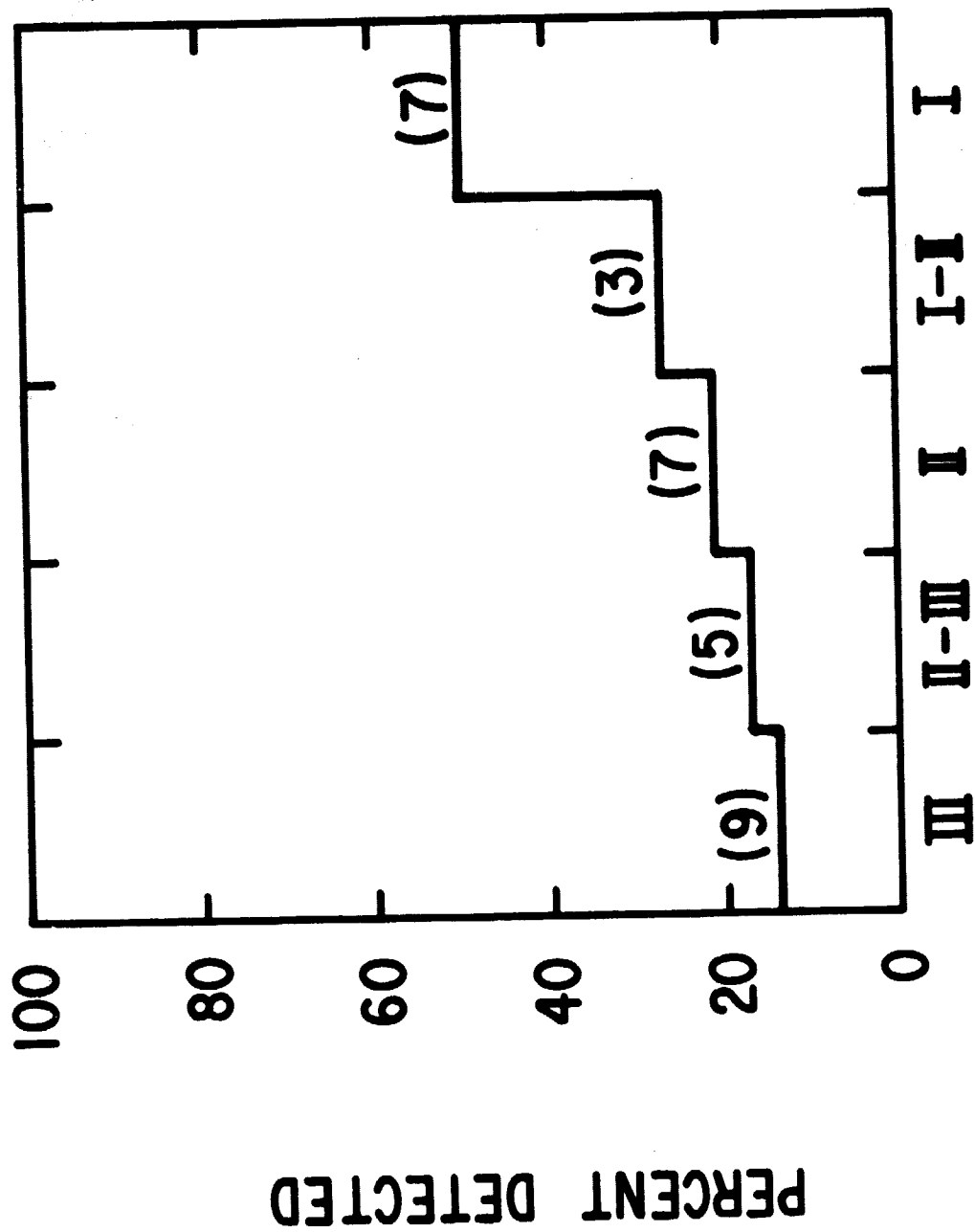
(1)	(2)	(3)	(4)	(5)	(6)	(7)	(8)	(9)	(10)	(11)	(12)
A262	027.79	035.81	028.54	036.67	026.44	035.95	026.71	035.02	029.09	035.76	1.75
A592	144.80	009.61	114.63	010.31	116.03	010.09	115.80	008.91	114.43	009.13	1.95
A644	123.52	-007.13	124.20	-006.42	122.86	-006.14	122.46	-007.58	123.80	-007.91	2.00
A754	136.56	-009.50	136.79	-009.32	136.02	-009.07	135.87	-009.54	136.64	-009.80	0.39
A2319	289.8	043.87	290.40	043.90	290.30	044.14	228.40	043.65	288.50	043.45	0.36
A2666	357.37	027.395	358.20	027.25	356.25	026.90	356.39	026.55	358.30	026.92	0.52

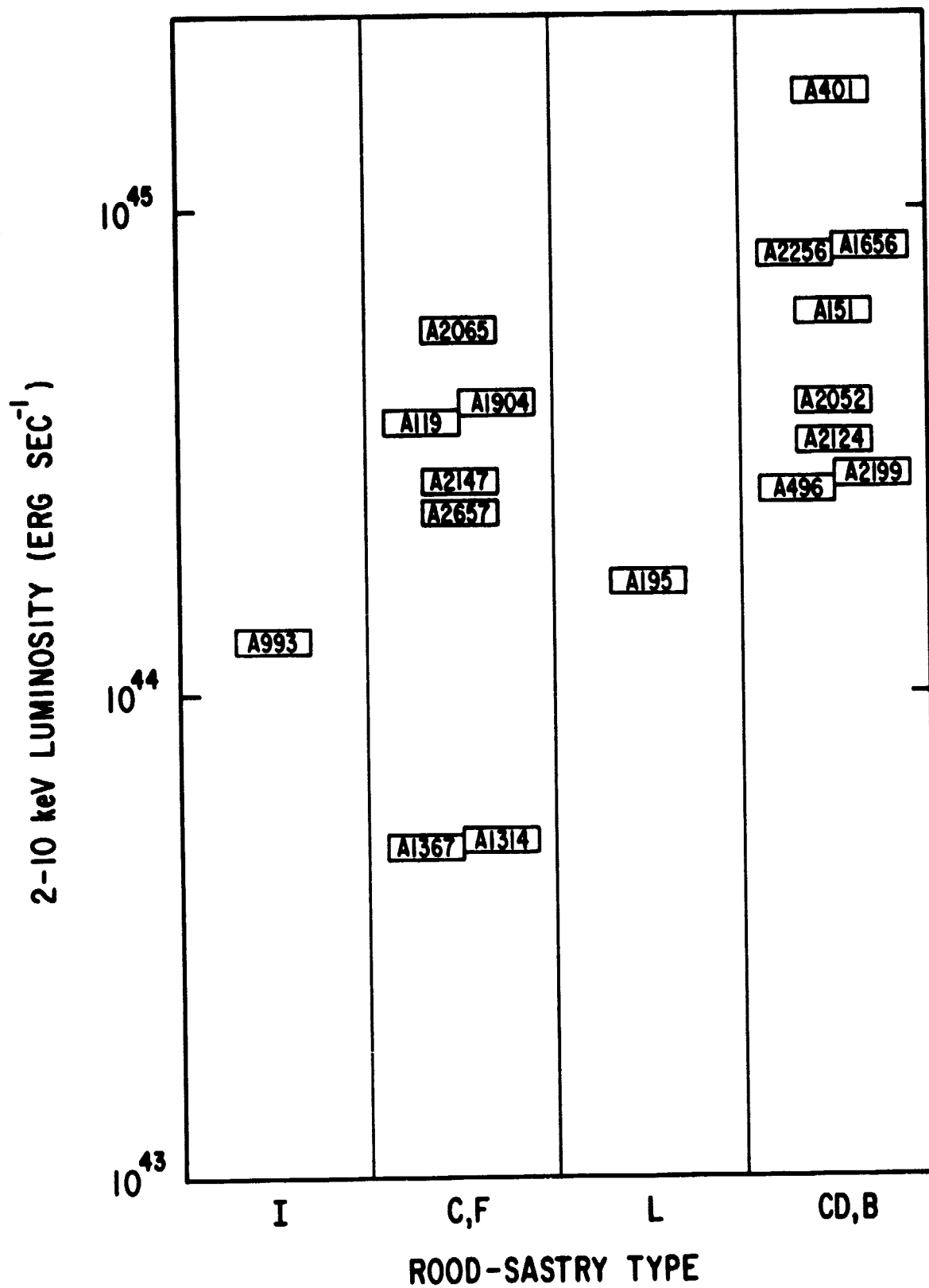


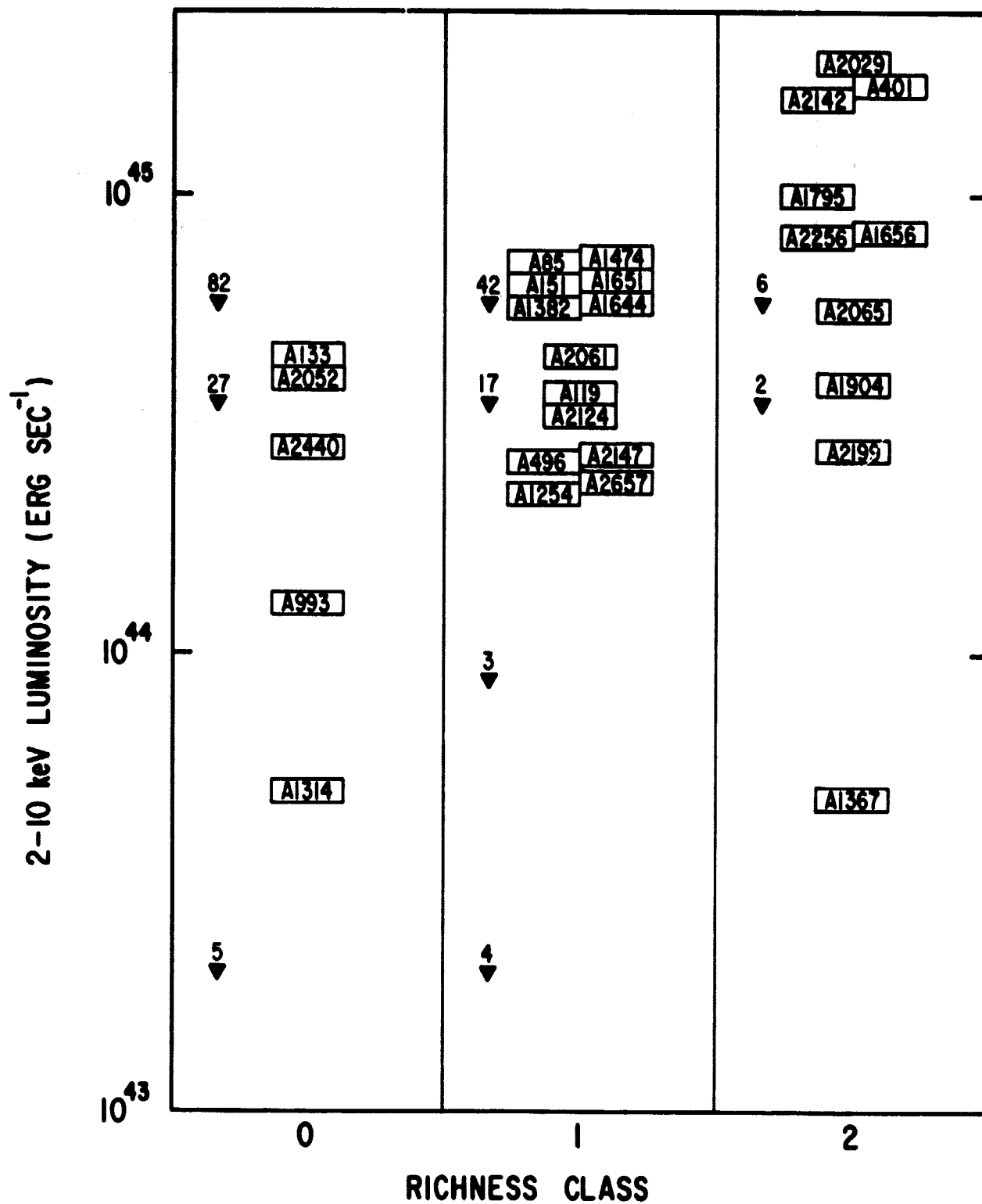
## FIGURE CAPTIONS

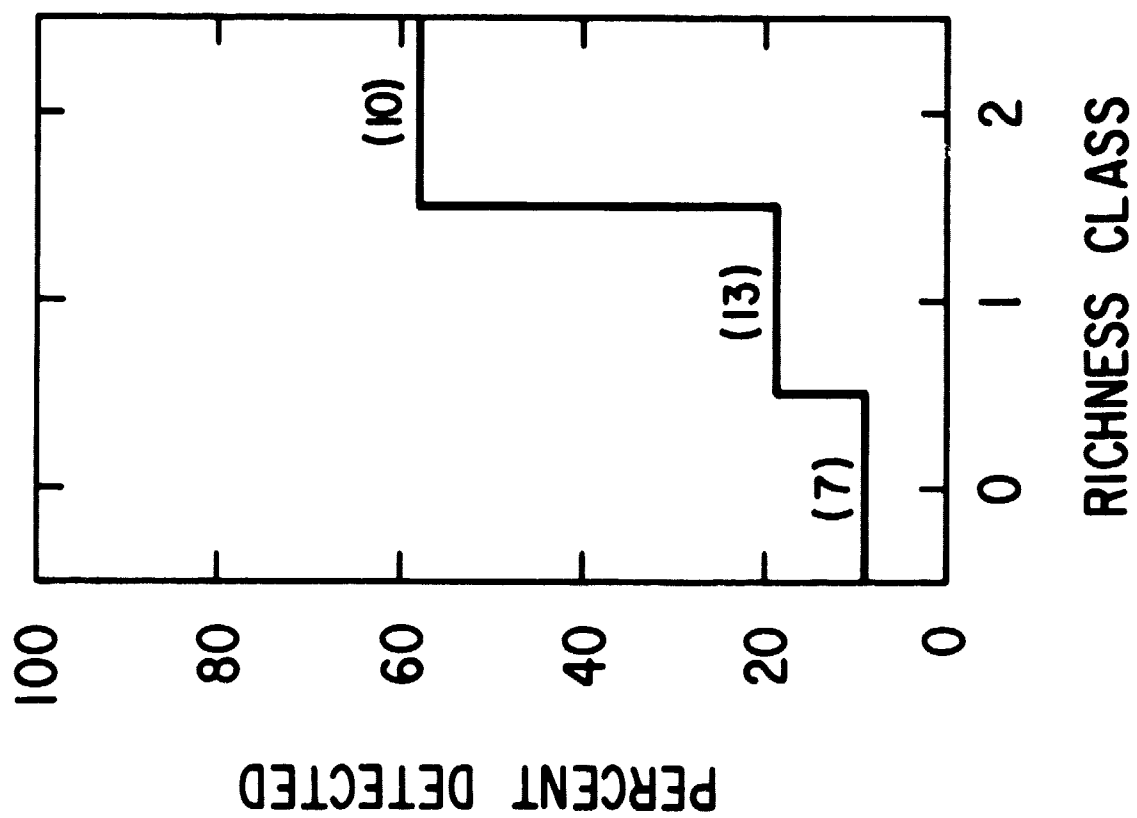
- Figure 1 - X-ray luminosity vs. Bautz-Morgan type for clusters brighter than 0.7 R15 counts. The estimated error in luminosity is 20% due to uncertainty in  $z$ . Richness class 2 clusters are in bold outlines; approximate upper limits for non-detections in distance classes 1-4 are indicated by arrow heads next to number represented.
- Figure 2 Percentage of detections as X-ray sources among the Bautz-Morgan classes. Brackets indicate number of actual detections.
- Figure 3 - X-ray luminosity versus Rood-Sastry type.
- Figure 4 - X-ray luminosity versus Abell richness class for clusters brighter than 0.7 R15. Three richness class 3 clusters were also in the sample, of which none were detected.
- Figure 5 - Percentage of detections as X-ray sources among the richness classes. Numbers in brackets indicate actual number detected.
- Figure 6 - 2-10 keV differential X-ray luminosity function.  $1\sigma$  error bars are shown, but are slightly misleading as this is a log-log plot. The dashed line is the best exponential fit.
- Figure 7 -  $\chi^2$  contours for the parameters of the exponential fit to the luminosity function. Contours for 68% and 90% confidence are shown. Minimum  $\chi^2$  is indicated by cross.
- Figure 8 - Comparison of HEAO A-2 integral luminosity function (solid points) with those from Ariel 5 (McHardy 1978) and Uhuru (Schwartz 1979). The dashed line represents the possible error due to the uncertain distance limits of  $D = 4$  clusters. The left hand box is plotted on a semi-log scale while the right hand box is log-log.



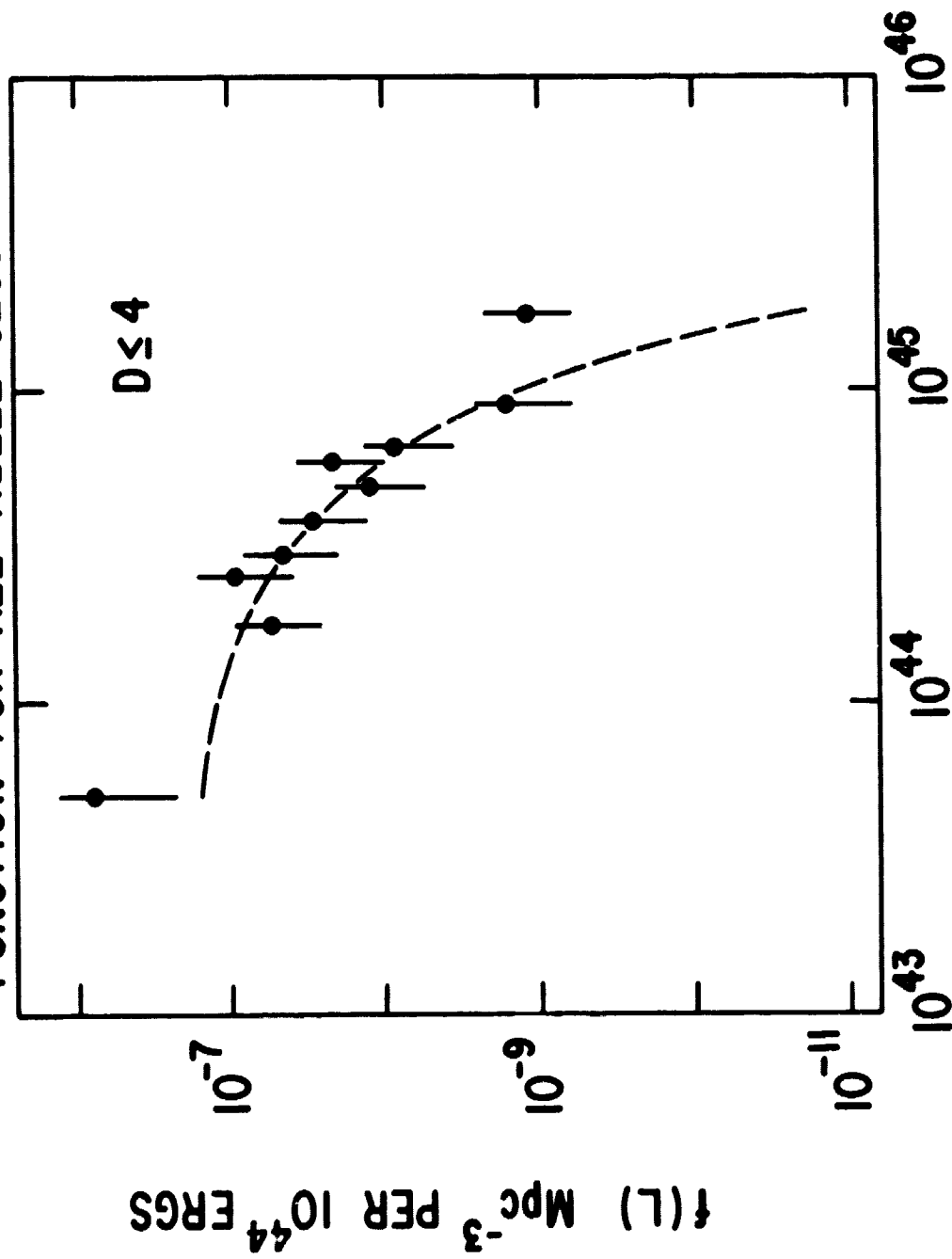




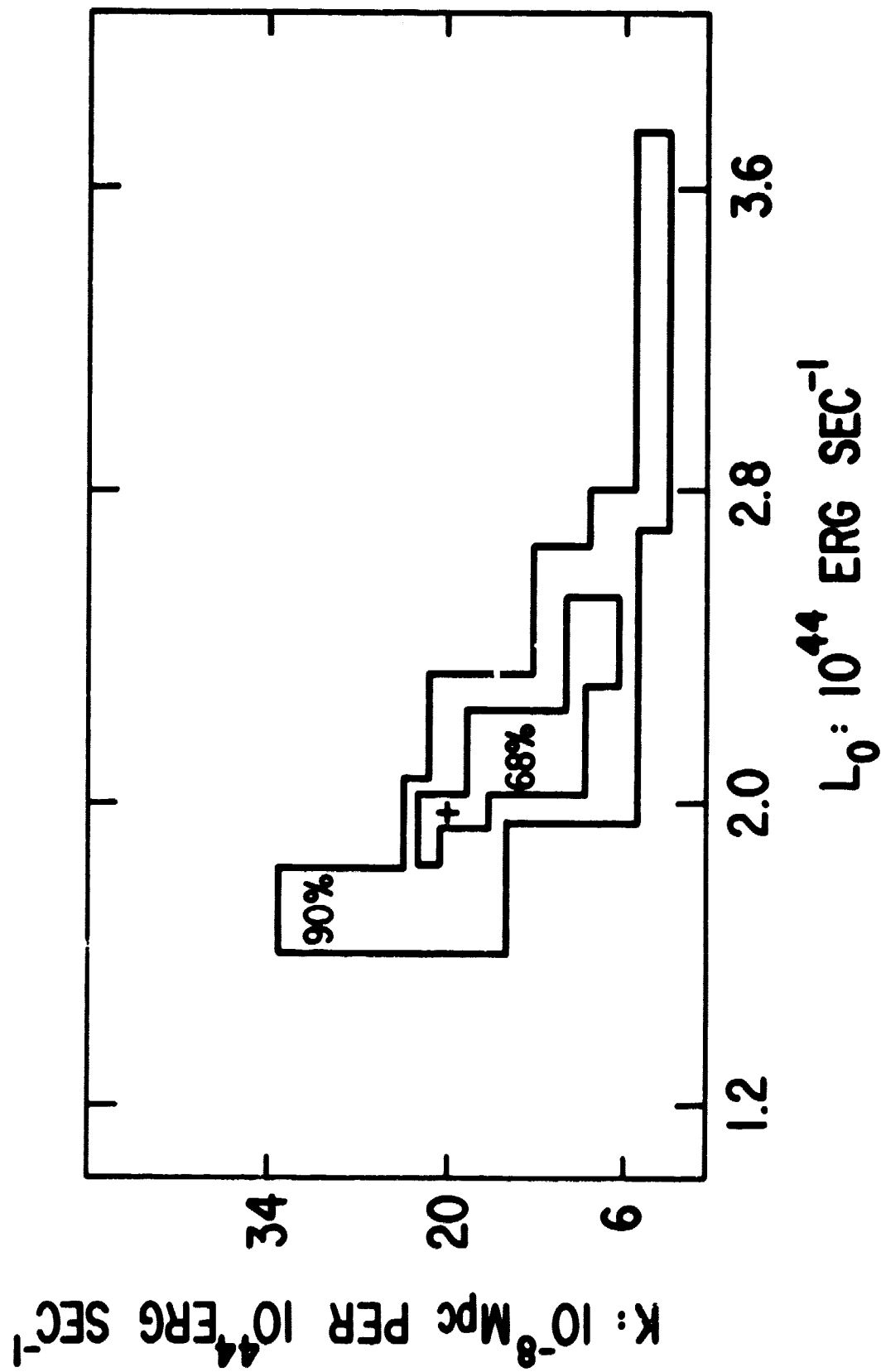




HEAD-A2 DIFFERENTIAL LUMINOSITY  
FUNCTION FOR ALL ABELL CLUSTERS

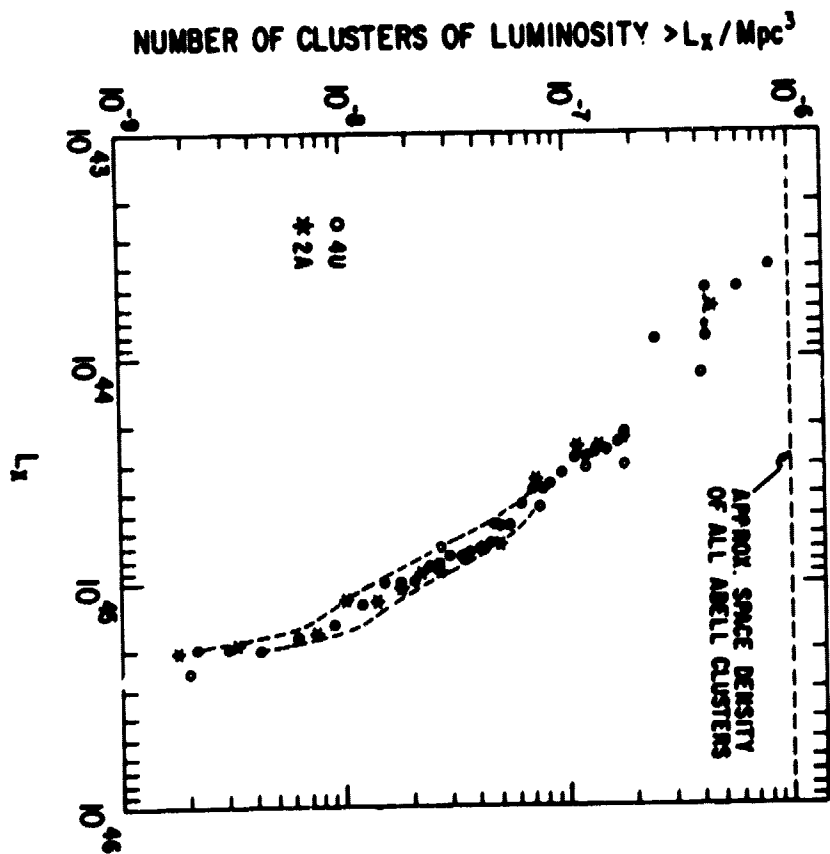
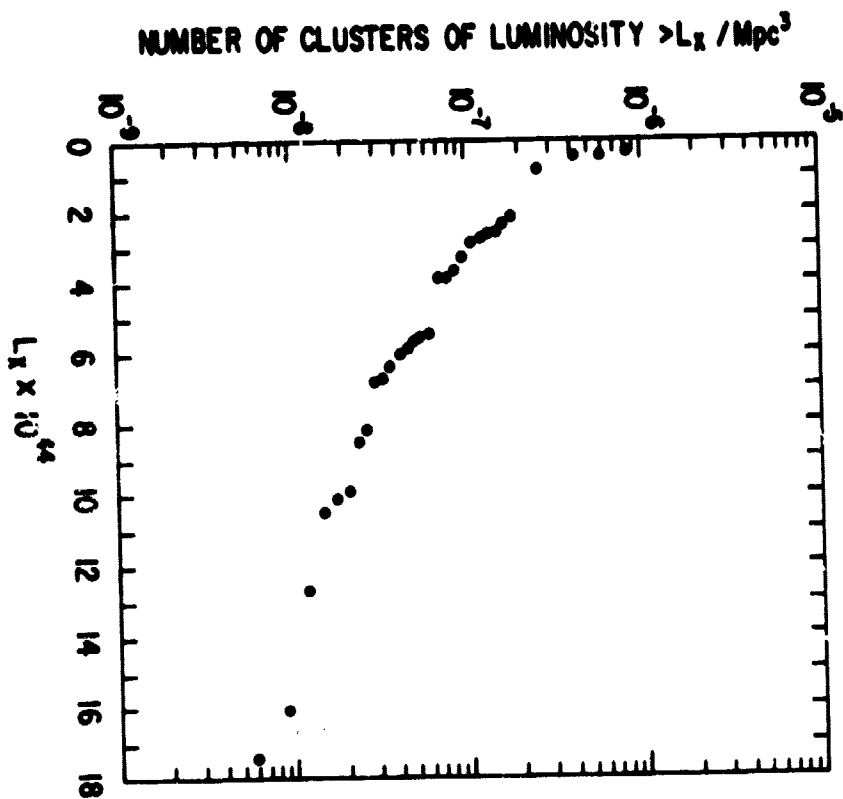


2-10 keV LUMINOSITY





# HEAD-I-A2 INTEGRAL LUMINOSITY FUNCTION OF CLUSTERS OF GALAXIES



Author addresses:

J.D. McKEE, Astronomy Program, Univ. of Maryland, College Park, MD 20742;

R.F. MUSHOTZKY, F.E. MARSHALL, E.A. BOLDT, S.S. HOLT, and P.J. SERLEMITSOS,  
Code 661, Laboratory for High Energy Astrophysics, NASA/Goddard Space Flight  
Center, Greenbelt, MD 20771;

S.H. PRAVDO, 320-47, Cal Tech, Pasadena, CA 91125